Eur. Phys. J. Appl. Phys. (2013) 64: 24505
DOI: 10.1051/epjap/2013120437

THE EUROPEAN PHYSICAL JOURNAL
APPLIED PHYSICS

Regular Article

Numerical modeling of electromagnetic waves scattering from 2D coastal breaking sea waves*

Refzul Khairi[1,a], Arnaud Coatanhay[1], Ali Khenchaf[1], and Yves Marie Scolan[2]

[1] Lab-STICC UMR CNRS 6285, ENSTA-Bretagne, rue Francois Verny, 29806 Brest cedex 9, France
[2] LBMS-DFMS EA 4325, ENSTA-Bretagne, rue Francois Verny, 29806 Brest cedex 9, France

Received: 2 October 2012 / Received in final form: 30 January 2013 / Accepted: 31 January 2013
Published online: 6 November 2013 –

Abstract. The aim of this work is to model the interaction of L-band electromagnetic waves with coastal breaking sea waves. The breaking sea waves' profiles are generated using the desingularized technique and the electromagnetic waves scattering is computed using the high-order method of moments (HO-MoM) combined with non uniform rational basis spline (NURBS) geometry. Our study mainly focuses upon the electromagnetic waves behavior in the crest and the cavity of breaking sea waves.

1 Introduction

In 2008, ENSTA-Bretagne, Telecom-Bretagne and IFREMER launched the marine opportunity passive systems (MOPS) project [1]. The objective of this project is to obtain the oceanographic information using electromagnetic waves scattering from coastal breaking sea waves. The sources of the electromagnetic waves in this case are the GNSS satellites (L-band passives electromagnetic waves sources) and the observation points are placed a dozen of meters above the sea surface (near field configuration) on the coast.

One of the MOPS project challenges is to model precisely the interaction of L-band electromagnetic waves with the breaking sea waves. The modeling involves two research domains: "hydrodynamic" to generate the breaking waves' profiles, and "electromagnetic" to compute the electromagnetic waves scattering.

The hydrodynamic theory shows that the presence and the evolution in time of the breaking sea waves depend on the sea floor slope. To model the breaking waves, different numerical approaches like finite element method, boundary integral method [2] or the long-tank model [3] can be used. In this work (see Sect. 2), we generate the breaking waves' profiles with the FSID (free area identification) code. A more relevant numerical solution based on a desingularized technique provides a robust and reliable simulation of highly nonlinear waves [4] in a shallow water context.

On the other hand, to model the electromagnetic waves scattering, we apply a boundary element method; meaning that first we compute the currents generated by incident waves and then, using these currents, we determine the waves scattering everywhere in the space. Unfortunately, it is well known that the standard boundary element approaches do not provide a reliable estimation for the electromagnetic fields scattered by breaking waves [5,6].

Indeed, the breaking sea waves' profiles have strong positive and negative curvatures and the standard MoM approaches raise convergence problems [7]. To compute the surface currents induced by these profiles, we propose to use the high-order method of moments (HO-MoM) combined with non uniform rational basis spline (NURBS) geometry. This technique will be presented in Section 3. Finally in Section 4, we show some simulation results which will be focused on the behavior of the electromagnetic waves in the crest and the cavity of breaking sea waves.

2 Breaking sea waves modeling

Sea wave is a complex physical phenomenon that involves nonlinear physics modeling. In many remote sensing applications, the sea surface is considered as a random physical system and its representation is given in terms of sea spectra: Pierson-Moskowitz, Elfouhaily, etc. These spectra give a statistical information of the sea surface's profile for a given location on ocean. However, the spectrum representation cannot give the information about the sea wave dynamics in general and the coastal breaking waves in particular. The hydrodynamic theory is required to respond to this problem.

The fundamental characteristic of coastal breaking waves is that their dynamics (and therefore their geometry) depend on the variation of the sea depth [8].

* Contribution to the Topical Issue "Numelec 2012", Edited by Adel Razek.

[a] e-mail: refzul.khairi@gmail.com

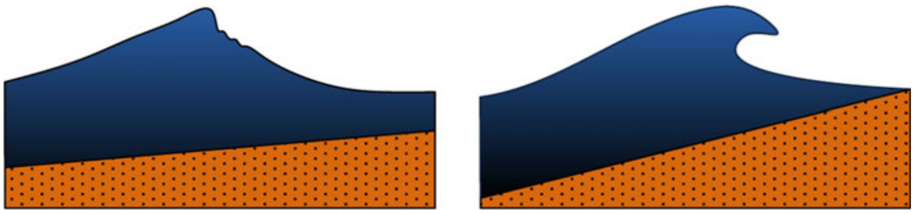

Fig. 1. Breaking waves types (i) spilling (ii) plunging.

When the waves approach the coast, the depth decreases rapidly and the waves reach their limit of stability then break, even for a small wind speed. Thus, the fluid mechanics imposes that the structure of the waves mainly depends on the slope of the coast bathymetry.

There are different classifications of breaking waves. These classifications are based on the form of the waves crest at their critical steepness. Galvin classified them into mainly two types: spilling and plunging [9]. Spilling waves occur when the ocean floor has a gradual slope. They break for a longer time than other waves and create relatively gentle waves. Plunging waves occur when the ocean floor is steep or has sudden depth changes, such as a reef or a sandbar. The crest of the plunging waves, which are much steeper than spilling ones, becomes vertical, overturns and hits the trough of the next wave, releasing most of its energy at once in a relatively violent impact. Figure 1 illustrates these two breaking waves types.

To model the movement of the breaking waves, the hydrodynamic theory is required. This theory is based on three fundamental equations: mass balance or continuity equation, momentum balance or Navier-Stokes equation and energy balance. To obtain solvable equations, we complete the previously cited ones by standard simplification hypotheses. In sea case, we can take the hypotheses that the fluid is ideal, incompressible and irrotational. These simplifications derive two principle equations in the breaking waves study: the Laplace equation

$$\nabla^2 \phi = 0 \tag{1}$$

and the Bernouilli equation

$$\frac{\partial \phi}{\partial t} + \frac{1}{2} |\nabla \phi|^2 + \frac{P}{\rho} + gz = 0, \tag{2}$$

where ϕ is the scalar velocity potential, ρ is the fluid density, P is the pressure and g is the gravity.

Applying the kinematic and dynamic boundary conditions in free surface and the floor of the waves, equations (1) and (2) can then be solved. The analytical solution for these equations is given by the theory of airy, stokes and cnoidal. However, these theories are limited to model the non-breaking waves. For the breaking waves case, the modeling by numerical methods is inevitable.

The numerical simulation of a breaking wave is still a challenge when dealing with a realistic three-dimensional sea state. The computational fluid dynamics do not provide yet efficient, robust and accurate tools. With no doubt, potential theory is the best framework in which the limit of stability of gravity waves can be reproduced. Three-dimensional configurations are still a challenge for industrial purposes, however two-dimensional configurations can be routinely simulated. Among the numerous numerical tools, the so-called desingularized technique is known to be very robust and does not suffer from drawbacks (like regridding and smoothing) of the standard boundary element methods. For the present applications, where both spilling and plunging breakers are modeled in combination with the influence of the bathymetry, there are even optimized techniques which make possible to implicitly account for solid boundaries. By using conformal mappings of the fluid domain, the time-varying problem can be formulated in terms of tracking markers on the free surface only. Those markers carry the information about the presence of impermeable frontiers (sea bottom, walls, ...). In practice, a succession of conformal transformations is used to turn the original physical fluid domain into a quarter (or half) space. The sketch in Figure 2 sums up these transformations.

From the physical z-plane (plus its symmetric part with respect to the left vertical wall), we "flatten" the two vertical walls (AB and FG) by using an integrable Schwartz-Christoffel transformation. Then the symmetric domain with respect to the horizontal axis is introduced. The local bathymetry is now a closed contour $CDE+sym.$ which is transformed by using successively a Karman-Trefftz transformation and a Theodorsen-Garrick transformation; we arrive at a unit circle which finally turns into a flat plate.

For the present two-dimensional potential flow, the Green function is of log type (Rankine source). This singularity and its six images with respect to the horizontal and vertical axes verify the initial boundary value problem except the boundary conditions on the free surface. The total velocity potential ϕ is thus expressed as a finite sum of these singularities denoted G

$$\phi(x, y, t) = \sum_{j=1}^{N} q_j(t) G(x, y, X_j(t), Y_j(t)), \tag{3}$$

where (X_j, Y_j) are the source location and q_j is the strength of source j. The singularities are located outside the fluid domain at a short distance from the actual free surface (desingularized technique). The velocity potential is updated by solving the dynamic (isobar surface) and kinematic (material surface) boundary conditions written in Lagrangian form

$$\frac{\mathrm{d}\phi}{\mathrm{d}t} = \frac{1}{2} (\nabla \phi)^2 - gY, \qquad \frac{\mathrm{d}X}{\mathrm{d}t} = \phi_{,x}, \qquad \frac{\mathrm{d}Y}{\mathrm{d}t} = \phi_{,y}, \tag{4}$$

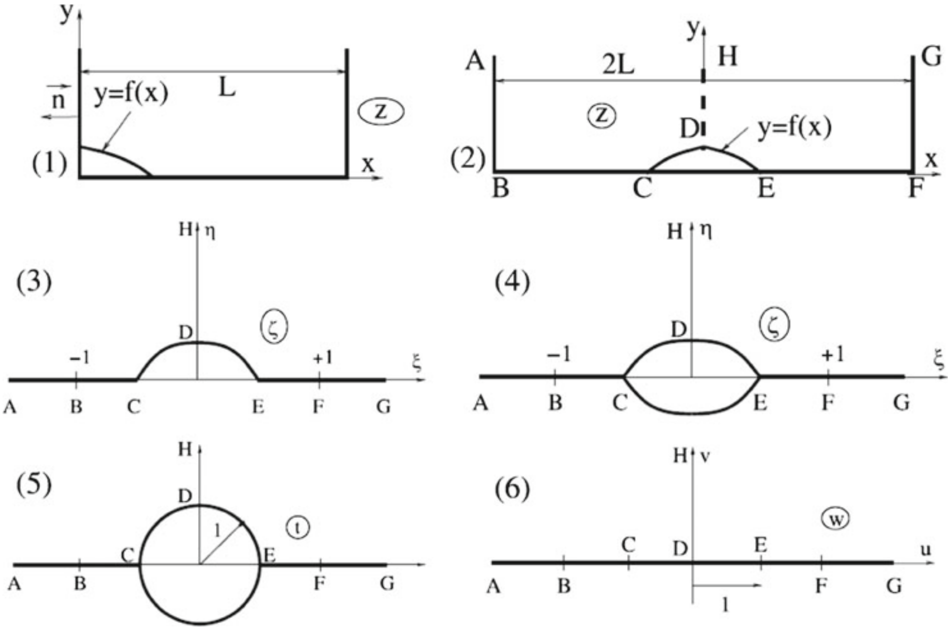

Fig. 2. Successive conformal transformations of the fluid domain.

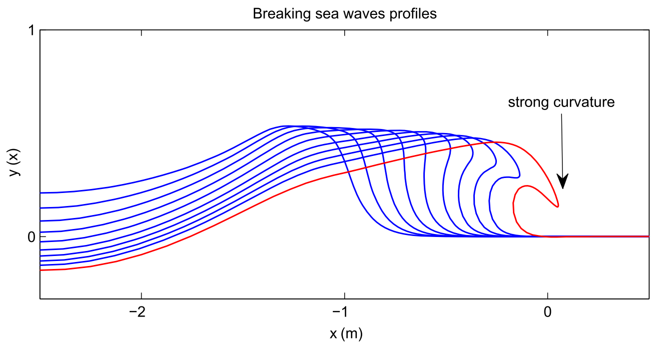

Fig. 3. Breaking waves profiles.

where g is the acceleration of gravity and (X, Y) are Lagrangian coordinates of a marker which moves with the fluid velocity $\nabla\phi = (\phi_{,x}, \phi_{,y})$. These algorithms are implemented in the code FSID (free surface identification), they are fully described in [4]. Here we use that code to produce realistic overturning crest and its dynamics as illustrated in Figure 3.

3 Electromagnetic waves scattering modeling

Once the breaking waves profiles are determined, we can compute the electromagnetic waves scattering from these profiles. The scattering problem can be seen as a special case of the radiation problems in which the sources (currents) are generated by the incident waves. Thus, the first step to solve the scattering problem is to find the currents. Once the currents are found, we can easily use the radiation equation to compute the field everywhere in the space.

At the boundary of the media, we can make a link between the incident waves and the surface currents. The boundary integral equations in this case are given respectively by the electric field integral equation (EFIE) and the magnetic field integral equation (MFIE):

$$\hat{n} \times \overline{E}^{\rm inc}(\overline{r}) = -\hat{n} \times \int \left\{ i\omega\mu \overline{J}_s G + \frac{1}{i\omega\epsilon} \left(\nabla' \cdot \overline{J}_s\right) \nabla' G \right\} {\rm d}\overline{r}', \tag{5}$$

$$\hat{n} \times \overline{H}^{\rm inc}(\overline{r}) = \frac{\overline{J}_s(\overline{r})}{2} - \hat{n} \times \int \overline{J}_s \times \nabla' G {\rm d}\overline{r}', \tag{6}$$

where $\overline{E}^{\rm inc}$ and $\overline{H}^{\rm inc}$ are the electric and magnetic incident waves, $\overline{J}_s$ are the surface currents, G is the Green function, μ is the magnetic permeability, ϵ is the electric permittivity, $\hat{n}$ is the normal vector to the surface, $\overline{r}$ and $\overline{r}'$ are the observation and source points.

Except for several canonical geometries like a cylinder or a sphere, the exact analytical solution does not exist for equations (5) and (6). For complex geometries, some simplification (asymptotic methods) can be made to approximate the exact solution. These methods are only valid for some types of surfaces and for some scattering mechanisms but do not remain accurate in general. However, they are still in great interest thanks to their small computation time. The other possibility is to use the numerical methods and more specifically the method of moments.

The method of moments (MoM) is a standard numerical technique to convert the integral equations into matrix linear systems. The procedure to apply the MoM involves three steps [10]:

- construction of the integral equations to present the systems,

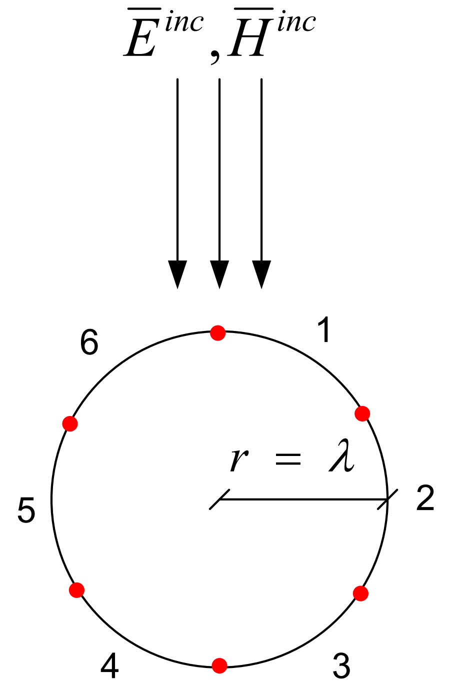

Fig. 4. Scattering from an infinitely long cylinder (circle).

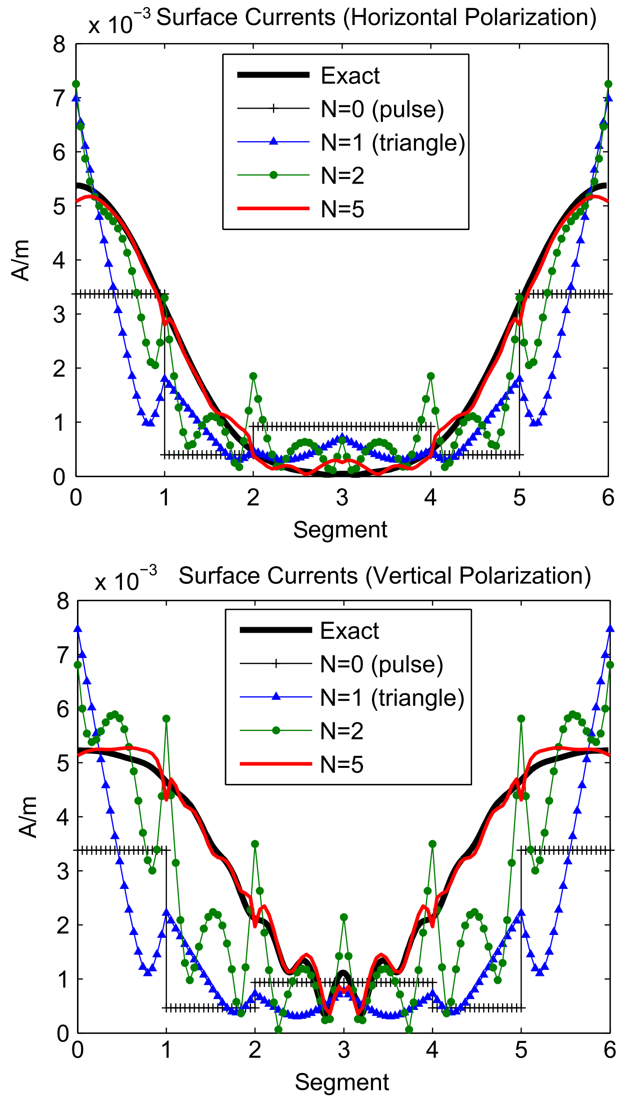

Fig. 5. Surface currents on infinitely long cylinder for horizontal and vertical polarizations.

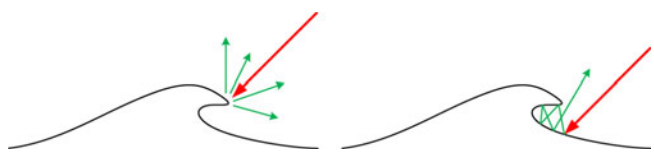

Fig. 6. Scattering from crest and cavity of the breaking waves.

– discretization of the integral equations into linear equation matrices using the basis and testing functions,
– solving the matrices equations to obtain the unknown coefficients.

The electromagnetic waves scattering systems are presented by the EFIE and MFIE. In general form, we can write:

$$\mathbf{S} = \mathcal{L}\mathbf{f}, \tag{7}$$

where $\mathbf{S}$ are the source functions (incident waves), $\mathcal{L}$ are the integral operators and $\mathbf{f}$ are the unknown functions (currents).

To discretize equation (7), the unknown functions $\mathbf{f}$ are approached by linear combination of the base functions $\mathbb{B}_b,\ b = 1, 2, \cdots, B$.

$$\mathbf{f} \approx \sum_{b=1}^{B} I_b \mathbb{B}_b, \tag{8}$$

where I_b are the unknown coefficients to be found. At the two sides of the equations, we introduce the testing functions $\mathbb{T}_a,\ a = 1, 2, \cdots, A$:

$$\langle \mathbb{T}_a, \mathbf{S} \rangle = \sum_{b=1}^{B} I_b \langle \mathbb{T}_a, \mathcal{L}\mathbb{B}_b \rangle . \tag{9}$$

Then we define the linear matrix equation as the following:

$$\mathbf{V} = \overline{\mathbf{Z}}\mathbf{I}. \tag{10}$$

The basis and testing functions have to be chosen in the same space as the unknown functions (Galerkin approach). In classical technique (Classic-MoM), one uses the pulse function if the continuity is not required (in 2D and 3D problems). The triangle (2D problems) and RWG/rooftop (3D problems) are used in the case the continuity is needed. These basis functions involve the discretization length in the order of $\lambda/10$. To increase this length, which means decreasing the unknown coefficient number, we can use the high-order polynomials as the basis (high-order method of moments (HO-MoM)). The high-order polynomials basis function can also improve the computation convergence.

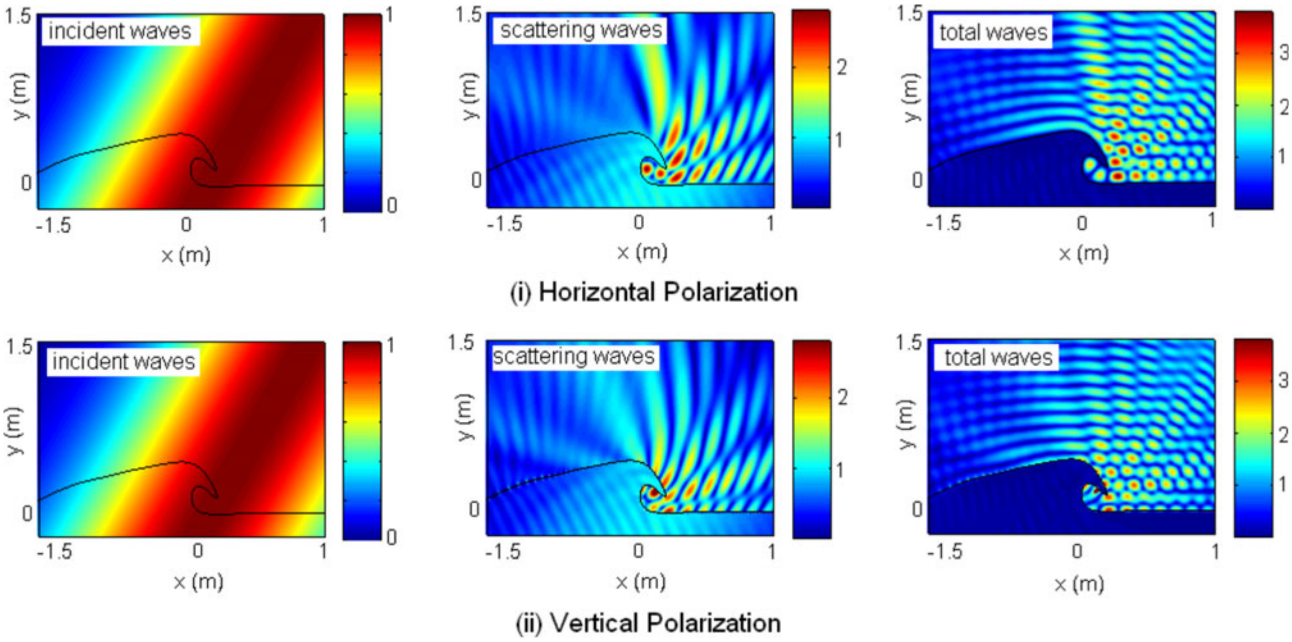

Fig. 7. Electromagnetic field scattering in crest and cavity.

The choice of the basis polynomials is based on two criteria: (1) they must allow the imposition of the continuity and (2) they have to be orthogonal to avoid the bad matrix condition. The Bernstein polynomials for example, fill in the first condition but not the second where the Legendre polynomials fill in the second but not the first. The modified Legendre polynomials constructed by Jorgensen fill these two conditions and are adopted in this work [11]. These polynomials are given by:

$$\mathbb{B} = \widetilde{L}_n(u) = \begin{cases} 1-u & n=0 \\ 1+u & n=1 \\ L_n(u) - L_{n-2}(u) & n \geq 2 \end{cases}, \qquad (11)$$

where L is the Legendre polynomials in the interval of u [11]. Two first terms of modified Legendre polynomials can be adjusted to impose the continuity and the higher-order terms are zero in the extremities.

Although the HO-MoM allows the use of the larger mesh-length than the Classic-MoM, this advantage cannot be exploited for the high-curvature objects which use the standard meshing-technique (linear segments). For these objects, we can use the non uniform rational basis splines (NURBS) meshing-technique. The use of NURBS in electromagnetic modeling is introduced by Spanish scientist [12] and its combination with HO-MoM can be found in recent articles [13,14].

To illustrate how HO-MoM + NURBS solve the electromagnetic scattering, we compute the surface currents on infinitely long cylinder (2D problem). The surface is discretized into six segments with the mesh-length $\mathrm{d}L = \lambda$, bigger than the standard one imposed by the classical MoM (Fig. 4). As reference, we take the analytical results (exact solution) in the form of the Hankel function series [15].

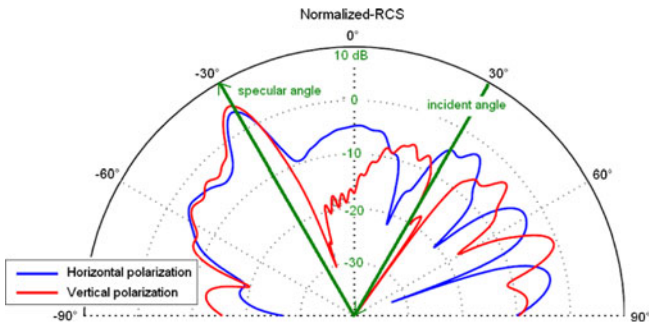

Fig. 8. Radar cross-section.

The surface currents for the horizontal and vertical polarizations are given in Figure 5. We see that the pulse and triangle basis function cannot approach the surface currents with given mesh-length. For the second order, there are big oscillations of the currents in the extremities of the mesh. Increasing the order of the basis functions (until fifth order in this example) can approach the exact currents and decreases the oscillation. From these surface currents, we can compute the field everywhere in the space.

4 Simulation results

The dispersal in the crest and the multiple reflection in the cavity are two main factors which influence the signature of electromagnetic waves scattering from breaking sea waves. These phenomena, shown in Figure 6, cannot be accurately modeled by asymptotic methods. For this reason, we use a numerical modeling. Since the breaking waves have a strong curvature, we use high-order method of moments combined with NURBS meshing-technique.

In this simulation, we compute the scattering and the total electromagnetic waves from the last profile of Figure 3. The incident waves angle is 30°. To avoid the artificial reflection at the edges due to the truncation of the surface, we use the tapered incident wave [16]. This is the incident wave which has a Gaussian-shaped footprint.

The electromagnetic waves for horizontal and vertical polarizations are presented in Figure 7. In these figures, the cavity resonance phenomenon clearly appears and the relative positions of the node and the anti-node in the different polarizations agree with the theoretical boundary conditions.

Finally, the distribution of energy is given by the radar cross-section (RCS). We see that the most part of energy is scattered into the specular directions (Fig. 8). However, the crest of the sea wave induces significant scattering in a large angular domain.

5 Conclusion

We have shown how a high-order method of moments (HO-MoM) combined with a non uniform rational basis spline (NURBS) geometry can compute precisely the electromagnetic wave scattering from breaking sea waves and can evaluate the electromagnetic field where the curvature of the profile is strong (crest for instance). This numerical approach generates numerical simulations of the electromagnetic scattering by a given breaking wave profile (Fig. 3) for the horizontal and vertical polarizations.

In the present study, the simulations are limited to the 2D problem and only co-polarization can be investigated. In future studies, we will introduce 3D breaking wave profiles to analyze the four components of the scattering matrix (co- and cross-polarization).

References

1. A. Coatanhay, R. Garello, B. Chapron, F. Ardhuin, in *Passive'08* (Hyères, France, 2008)
2. Q. Ma (Ed.), in *Advances in Numerical Simulation of Nonlinear Water Waves* (World Scientific, London, UK, 2010)
3. P. Wang, Y. Yao, M.P. Tulin, Int. J. Numer. Methods Fluids **20**, 1315 (1995)
4. Y.M. Scolan, J. Fluids Struct. **26**, 918, 2010
5. J.C. West, IEEE Trans. Antennas Propag. **37**, 2725 (1999)
6. J.C. West, Z. Zhao, IEEE Trans. Antennas Propag. **40**, 583 (2002)
7. C. Davis, K. Warnick, IEEE Trans. Antennas Propag. **53**, 321 (2005)
8. R.M. Sorensen, *Basic Coastal Engineering* (Springer, New York, USA, 2006)
9. C.J. Galvin, J. Geophys. Res. **73**, 3651 (1968)
10. M. Sadiku, *Numerical Techniques in Electromagnetics with MATLAB* (CRC Press, Boca Raton, USA, 2009)
11. E. Jorgensen, J.L. Volakis, P. Meincke, O. Breinbjerg, IEEE Trans. Antennas Propag. **52**, 2985 (2004)
12. L. Valle, F. Rivas, M.F. Catedra, IEEE Trans. Antennas Propag. **42**, 373 (1994)
13. H. Yuan, N. Wang, C. Liang, IEEE Trans. Antennas Propag. **57**, 3558 (2009)
14. Z.L. Liu, J. Yang, Progress Electromagn. Res. **96**, 83 (2009)
15. W. Gibson, *The Method of Moments in Electromagnetics* (Chapman & Hall/CRC, Boca Raton, USA, 2008)
16. H. Braunisch, Y. Zhang, C. Ao, S. Shih, Y. Yang, K. Ding, J. Kong, L. Tsang, IEEE Trans. Antennas Propag. **48**, 1086 (2000)